Dynamic bimodality of curli expression in planktonic cultures of *Escherichia coli* is stabilized by cyclic-di-GMP regulation

Olga Lamprecht[1†], Maryia Ratnikava[1], Paulina Jacek[1], Eugen Kaganovitch[1], Nina Buettner[1], Kirstin Fritz[1], Robin Köhler[1], Julian Pietsch[1], and Victor Sourjik[1*]

[1]Max Planck Institute for Terrestrial Microbiology and Center for Synthetic Microbiology (SYNMIKRO), Karl-von-Frisch Strasse 16, 35043 Marburg, Germany

[†]Present address: Eawag: Swiss Federal Institute of Aquatic Science and Technology, Dübendorf, Switzerland

*Corresponding author: Victor Sourjik, victor.sourjik@synmikro.mpi-marburg.mpg.de

Abstract

Curli amyloid fibers are major constituent of the extracellular biofilm matrix formed by bacteria of the Enterobacteriaceae family. Within *Escherichia coli* biofilms, curli gene expression is limited to a subpopulation of bacteria, leading to heterogeneity of extracellular matrix synthesis. Here we show that bimodal activation of curli expression also occurs in well-mixed planktonic cultures of *E. coli*, resulting in stochastic differentiation into distinct subpopulations of curli-positive and curli-negative cells at the entry into the stationary phase of growth. Monitoring curli activation in individual *E. coli* cells growing in a microfluidic device revealed that the curli-positive state is only metastable and it can spontaneously revert during continuous growth in a conditioned medium. The regulation by c-di-GMP is not required for curli gene activation or for differentiation of *E. coli* in subpopulations of curli-producing and curli-negative cells. Instead, we observe that c-di-GMP modulates the probability and dynamics of stochastic curli activation and enhances stability of the curli-positive state.

Keywords: Gene expression, bacteria, biofilm, bistability, differentiation, amyloid fibers

Introduction

Curli amyloid fibers are the key component of the extracellular matrix produced during biofilm formation by *Escherichia coli*, *Salmonella enterica*, and other Enterobacteriaceae [1-9]. In *E. coli* and *S. enterica* serovar Typhimurium, curli genes are organized in two divergently transcribed *csgBAC* and *csgDEFG* operons that share a common intergenic regulatory region [10]. Expression of these operons is under regulation of the stationary phase sigma factor σ^S (RpoS) and thus becomes activated during the entry into the stationary phase of growth [4, 11-14]. This activation is achieved by the σ^S-dependent induction of the transcriptional regulator CsgD, which then controls the expression of the *csgBAC* operon that encodes the major curli subunit CsgA along with the curli nucleator CsgB and the chaperone CsgC [7, 8, 15]. In turn, *csgD* expression in *E. coli* and *S.* Typhimurium is either directly or indirectly regulated by multiple cellular factors that mediate responses to diverse environmental changes, including both global and specific transcriptional regulators, small regulatory RNAs and second messengers (reviewed in [16-19]).

One of the key regulators of *csgD* is the transcription factor MlrA [13, 14, 20, 21]. The activity of MlrA depends on cellular levels of bacterial second messenger bis-(3'-5')-cyclic dimeric guanosine monophosphate (c-di-GMP), and in *E. coli* this control is known to be mediated by a pair of the interacting diguanylate cyclase (DGC) and phosphodiestherase (PDE) enzymes, DgcM and PdeR, that form a ternary complex with MlrA [12, 14, 22]. MlrA is kept inactive by binding PdeR, and this interaction is relieved when the latter becomes active as a PDE thus acting as the trigger enzyme [22, 23]. This inhibition is counteracted by DgcM that locally produces c-di-GMP to engage PdeR, as well as by the global pool of c-di-GMP. Besides its enzymatic activity, DgcM might also activate MlrA through direct protein interaction. Another DGC-PDH pair, DgcE and PdeH, provides global regulatory input into the local DgcM-PdeR-MlrA regulation [12, 24].

Previous studies of *E. coli* macrocolony biofilms formed on agar plates showed that curli expression occurs in the upper layer of the colony, but even in this layer its expression remained heterogeneous [25-27], indicating an interplay between global regulation of curli gene expression by microenvironmental gradients within biofilms and its inherent stochasticity. Differentiation of *E. coli* into distinct subpopulations of cells either expressing or not expressing curli was also observed in submerged biofilms formed in liquid cultures, whereby curli expression was associated with cellular aggregation [28]. Furthermore, bi- or multimodality of *csgD* reporter activity was also observed in the early stationary phase among planktonic cells in *S.* Typhimurium [29, 30] and *E. coli* [27]. Given established c-di-GMP-dependent regulation of CsgD activity, it was proposed that bistable curli expression originates from a toggle switch created by mutual inhibition between DgcM and PdeR, which could act as a bistable switch [27, 31].

In this study we demonstrate that stochastic differentiation of *E. coli csgBAC* operon expression into distinct subpopulations of curli-positive and -negative cells occurs during the entry into the stationary phase in a well-stirred planktonic culture, and thus in absence of any environmental gradients. Similar stochastic and reversible differentiation could be observed among cells growing in conditioned medium in the microfluidic channel. The upstream regulation by c-di-GMP is not required to establish the bimodality of curli expression, but it determines the fraction of curli-positive cells and enhances the stability of curli activation.

Materials and methods

Bacterial strains and plasmids

All strains and plasmids used in this study are listed in Table S1. Derivative of *E. coli* W3110 [26] that was engineered to encode a chromosomal transcriptional sfGFP reporter downstream of the *csgA* gene [28] (VS1146) was used here as the wildtype strain. Gene deletions were obtained with the help of P1 phage transduction using strains of the Keio collection [32] as donors, and kanamycin resistance cassette was removed using FLP recombinase [33]. For expression, *dgcE* and *pdeH* genes were cloned into pTrc99A vector [34].

Growth conditions for planktonic cultures

Planktonic *E. coli* cultures were grown in tryptone broth (TB) medium (10 g tryptone, 5 g NaCl per liter), supplemented with antibiotics where necessary. Overnight cultures grown at 30°C were diluted 1:100, unless indicated otherwise, in 5-10 ml of fresh TB and grown at 30°C at 200 rpm in 100 ml flasks in a rotary shaker until indicated OD_{600} or overnight (18-25 h; OD_{600} ~ 1.3-1.8). Alternatively, cultures were grown in 96-well plates with linear shaking in a plate reader, with 200 µl culture per well. Where indicated, bacterial cultures were supplemented with either 1 mM L-serine (after 6 h of growth) or 0.1–10 mg/l DL-serine hydroxamate at inoculation.

Growth and quantification of submerged biofilms

Submerged biofilms were grown and quantified as described previously [28], with minor modifications. Overnight bacterial cultures grown in TB were diluted 1:100 in fresh TB medium and grown at 200 rpm and 30°C in a rotary shaker to OD_{600} of 0.5. These cultures were then diluted in fresh TB medium to a final OD_{600} of 0.05, and 300 µl was loaded onto a 96-well plate (Corning Costar, flat bottom; Sigma-Aldrich, Germany) and incubated without shaking at 30°C for 46 h.

For quantification of biofilm formation, the non-attached cells were removed and the wells were washed once with phosphate-buffered saline (PBS; 8 g NaCl, 0.2 g KCl, 1.44 g Na_2HPO_4, 0.24 g KH_2PO_4). Attached cells were fixed for 20 min with 300 µl of 96% ethanol, allowed to dry for

40 min, and stained with 300 µl of 0.1% crystal violet (CV) solution for 15 min at room temperature. The wells were subsequently washed twice with 1x PBS, incubated with 300 µl of 96% ethanol for 35 min and the CV adsorption was measured at OD_{595} using INFINITE M NANO^{+} plate reader (Tecan Group Ltd., Switzerland). These CV values were normalized to the OD_{600} values of the respective biofilm cultures.

Macrocolony biofilm assay

Macrocolony biofilms were grown as described previously [26]. Briefly, 5 µl of the overnight liquid culture grown at 37°C in lysogeny broth (LB) medium (10 g tryptone, 10 g NaCl, and 5 g yeast extract per liter) was spotted on salt-free LB agar plates supplemented with Congo red (40 µg/ml). Plates were incubated for 8 days at 28°C.

Fluorescence measurements

Measurements of GFP expression in an INFINITE M1000 PRO plater reader (Tecan Group Ltd., Switzerland) were done using fluorescence excitation at 483 nm and emission at 535 nm. Relative fluorescence was calculated by normalizing to corresponding OD_{600} values of the culture.

For fluorescence measurements using flow cytometry, aliquots of 40-300 µl of liquid bacterial cultures were mixed with 2 ml of tethering buffer (10 mM KH_2PO_4, 10 mM K_2HPO_4, 0.1 mM EDTA, 1 µM L-methionine, 10 mM lactic acid, pH 7.0). Macrocolonies were collected from the plate, resuspended in 10 ml of tethering buffer and then aliquots of 40 µl were mixed with 2 ml of fresh tethering buffer. Samples were vigorously vortexed and then immediately subjected to flow cytometric analysis using BD LSRFortessa Sorp cell analyzer (BD Biosciences, Germany) using 488-nm laser. In each experimental run, 50,000 individual cells were analyzed. Absence of cell aggregation was confirmed by using forward scatter (FSC) and side scatter (SSC) parameters. Data were analyzed using FlowJo software version v10.7.1 (FlowJo LLC, Ashland, OR, US), applying a software-defined background fluorescence subtraction.

Microfluidics

Conditioned medium was prepared by cultivating wildtype *E. coli* in TB in a rotary shaker at 30°C for 20 h, after which the cell suspension was centrifuged at 4000 rpm for 10 min, medium was filter-sterilized and stored at 4°C. Mother machine [35] microfluidics device was designed, fabricated and operated as described in Supporting protocols. *E. coli* cells from the overnight culture in TB were loaded into the mother machine growth sites by manual infusion of the cell suspension through one of the two inlets using a 1-ml syringe. Cells were first allowed to grow at 30 °C for 4 h in fresh TB, then switched to the conditioned TB and cultivated for up to 26 h. Phase contrast and GFP fluorescence images were acquired using a Nikon Eclipse Ti-E

inverted microscope with a time interval of 10 min. Details of image analysis are described in Supporting protocols.

Results

Bimodal curli expression is induced in planktonic culture

In order to characterize curli expression in planktonic culture of *E. coli*, we followed the induction of chromosomal transcriptional reporter of *csgBAC* operon, where the gene encoding for green fluorescent protein (GFP) was cloned with a strong ribosome binding site as a part of the same polycistronic RNA downstream of *csgA* [28]. In our previous study of submerged *E. coli* biofilms, this reporter showed bimodal expression both in the surface-attached biofilm and in the pellicle at the liquid-air interface [28]. When *E. coli* culture was grown at 30°C in tryptone broth (TB) liquid medium, this reporter became induced during transition to the stationary phase (Figure 1A), which is consistent with previous reports [12, 14]. The observed induction of curli expression occurred at similar density in the cultures with different initial inoculum size. In both cases the onset of induction apparently coincided with the reduction of the growth rate, which likely occurs due to depletion of amino acids in the medium and induction of the stringent response [36, 37], consistent with proposed role of stringent response in the regulatory cascade leading to curli gene expression [18, 23]. In agreement with that, curli expression was strongly reduced when *E. coli* culture was grown in a concentrated TB medium (Figure S1A) or when TB medium was supplemented with serine (Figure S2A). Moreover, the induction of curli reporter was strongly enhanced by addition of serine hydroxamate (SHX), which is known to mimic amino acid starvation and induce stringent response [38] (Figure S2A).

In order to investigate whether curli expression was uniform or heterogeneous across planktonic *E. coli* population, we next measured curli reporter activity in individual cells using flow cytometry. The reporter was induced only in a fraction of cells, and this bimodality of curli expression became increasingly more pronounced at later stages of culture growth, reaching its maximum in the overnight culture (Figure 1B). Thus, the bimodal induction of curli gene expression is observed not only in biofilms but also in a well-mixed planktonic culture. While curli activation was more pronounced in a cell culture growing in an orbital shaker (Figure 1B), bimodality was also observed during culture growth in the plate reader (Figure S1B). Notably, stimulation of curli expression by SHX or its suppression by additional nutrients affected the fraction of positive cells rather than their expression levels (Figure S1B and Figure S2B).

Bimodality of curli expression does not require regulation by c-di-GMP

Subsequently, we investigated dependence of curli expression in planktonic culture on the upstream regulation by c-di-GMP (Figure 2A). As expected, no activation of curli reporter was

observed in the absence of MlrA (Figure 2B). Curli expression was also affected by the lack of enzymes that control MlrA activity at the global (DgcE and PdeH) or local (DgcM and PdeR) level of c-di-GMP regulation (Figure 2C). Consistently with their established regulatory roles, deletions of cyclase genes *dgcE* and *dgcM* resulted in nearly all cells being curli-negative, whereas deletions of diesterase genes *pdeH* and *pdeR* led to activation of curli expression in the majority of cells within the planktonic population. Notably, in all cases a small fraction of positive (for cyclase knockouts) or negative (for esterase knockouts) cells could be detected, indicating that neither of these knockouts entirely eliminates the bimodality of curli expression. This conclusion could be further confirmed by combined deletions of cyclase and diesterase genes. Removal of the entire global level of c-di-GMP regulation in Δ*pdeH* Δ*dgcE* strain led to a bimodal pattern of curli activation (Figure 2D) that was similar to that observed in the wildtype cells. Even more surprisingly, the distribution of curli expression remained bimodal upon removal of the local level of c-di-GMP regulation in Δ*pdeR* Δ*dgcM* strain, although the fraction of curli-positive cells was reduced and heterogeneity of their expression levels increased in this background. The bimodality of curli expression was also retained in the quadruple knockout strain lacking all four cyclase and diesterase genes (Figure 2E). Thus, whereas both global and local c-di-GMP-dependent regulation of MlrA activity clearly affect the fraction of curli-positive cells, they are apparently not required to activate curli expression or to establish its bimodality in the planktonic cell population.

Vibrio cholerae transcriptional regulator VpsT, a close homologue of CsgD, has been shown to be directly regulated by binding to c-di-GMP [39]. Furthermore, in *S.* Typhimurium c-di-GMP was proposed to regulate *csgD* expression not only at transcriptional but also at a posttranscriptional level [40]. We thus aimed to verify that *E. coli* curli gene expression was no longer sensitive to the global cellular level of c-di-GMP in the absence of the local PdeR/DgcM regulatory module. Indeed, whereas the overexpression of c-di-GMP cyclase DgcE or phosphodiesterase PdeH had strong impacts on the fraction of curli-positive cells in the wildtype, the quadruple mutant was insensitive to such overexpression (Figure S3), confirming that in this background the expression of the *csgBAC* reporter is no longer affected by the global pool of c-di-GMP.

Curli activation shows higher variability in absence of c-di-GMP regulation

We next explored how the fraction of curli-positive cells in the population depends on the conditions of culture growth, with and without regulation by c-di-GMP. As mentioned above, even in the wildtype strain the fraction of curli-positive cells was smaller in cultures grown in multi-well plates (Figure S1B) compared to the incubation in the flask in an orbital shaker (Figure 1B). However, this reduction in the number of curli-positive cells was much more pronounced for Δ*pdeR* Δ*dgcM* or Δ*pdeH* Δ*dgcE* Δ*pdeR* Δ*dgcM* strains, where only a small

fraction of cells became positive under these growth conditions (Figure 3A,B and Figure S4). Also individual *dgc* and *pdh* gene knockout strains showed reduced activation of curli reporter (Figure S4). Of note, another difference with the flask culture was that the low-fluorescence peak of the wildtype culture was not fully negative but apparently contained a large fraction of cells with incompletely activated curli reporter, which could also be seen in Δ*pdeH* or Δ*pdeR* knockouts but not in the Δ*pdeH* Δ*dgcE* Δ*pdeR* Δ*dgcM,* Δ*pdeR* Δ*dgcM* or Δ*pdeH* Δ*dgcE* strains (Figure 3B and Figure S4). Similar results were obtained even upon prolonged incubation in the plate reader (Figure S5), confirming that the observed difference with the overnight flask culture was not because of the different growth stage.

We further tested reporter activation under growth conditions that favour biofilm formation. During formation of static submerged biofilms in multi-well plates where cultures are grown without shaking, the overall curli activation in the populations of Δ*pdeH* Δ*dgcE*, Δ*pdeR* Δ*dgcM* or Δ*pdeH* Δ*dgcE* Δ*pdeR* Δ*dgcM* cells (Figure 3C) as well as in the individual knockout strains (Figure S6A) was comparable to that in the culture grown in the orbital shaker (Figure 2B-E). Curli gene activation in individual mutant strains correlated well with the levels of submerged biofilm formation (Figure S6B), although the lack of regulation by c-di-GMP resulted in stronger reduction of the biofilm biomass, consistent with other roles of c-di-GMP in biofilm formation besides curli regulation.

We also grew all strains in the form of macrocolony biofilms on an agar plate [26]. Interestingly, here the extent of reporter activation in the Δ*pdeR* Δ*dgcM* and Δ*pdeH* Δ*dgcE* Δ*pdeR* Δ*dgcM* strains was much higher and comparable to that of the wildtype (Figure 3D) and even individual Δ*dgcE* and Δ*dgcM* knockouts showed high fraction of curli-positive cells (Figure S7A), consistent with their stronger Congo red staining compared to the Δ*mlrA* negative control (Figure S7B). Summarily, these results confirm that the regulation by c-di-GMP is not required for (bimodal) curli activation, but also suggest that in absence of this control the fraction of culri-positive cells is more sensitive to growth conditions.

Curli activation is a stochastic and reversible process stabilized by c-di-GMP

In order to investigate the dynamics of curli activation, and the effects of c-di-GMP regulation, at the single-cell level, we utilized “mother machine”, a microfluidic device where growth of individual bacterial cell lineages could be followed in a highly parallelized manner over multiple generations [35] (Figure 4, Figure S8 and Supporting protocols). To activate curli expression in continuously growing single cells by mimicking nutrient depletion, *E. coli* wildtype or Δ*pdeH* Δ*dgcE* Δ*pdeR* Δ*dgcM* cells were first loaded into the mother machine from the overnight culture, allowed to grow in fresh TB medium for several generations and then shifted to the TB medium that was pre-conditioned by growing the batch culture (see Materials and Methods and Supporting protocols). For both strains, a fraction of curli-positive cells was observed at

the beginning of the experiment since cells originated from the overnight culture, but all cells turned off curli expression after resuming exponential growth in the fresh medium (Figure 4A,B, Figure S9, Figure S10, Figure S11, Movie S1 and Movie S2). Following shift to the conditioned medium, cell growth rate was strongly reduced (Figure 4A,C,E and Figure S9A) to approximately the same low growth rate for both strains. After several generations of slow growth in the conditioned medium, individual cells of both strains activated curli expression, while other cells remained in the curli-off state (Figure 4A,C and Figure S11). Importantly, we observed that after several generations in the curli-on state, individuals cells of both strains turned curli expression off again during continuous growth in the conditioned medium (Figure 4B,D and Figure S10), and in some cases there was even a second activation event.

Despite these overall similarities, the dynamics of curli reporter activation showed several differences between the wildtype and the Δ*pdeH* Δ*dgcE* Δ*pdeR* Δ*dgcM* strain. Most clearly, the rate of curli activation in individual cells was apparently higher in absence of the c-di-GMP regulation (Figure 4B,D,F, Figure S10, Figure S12 and Figure S13). Additionally, the induction showed greater intercellular heterogeneity in the Δ*pdeH* Δ*dgcE* Δ*pdeR* Δ*dgcM* strain (Figure 4F, Figure S10, Figure S12 and Figure S13). Thus, the control of curli expression by c-di-GMP reduces the rate but increases the stability of curli induction.

Discussion

Expression of the curli biofilm matrix genes is known to be heterogeneous or even bistable in communities of *E. coli* [25-28] and *S.* Typhimurium [29, 30], which might have important functional consequences for the biomechanics of bacterial biofilms [27] and for stress resistance and virulence of bacterial populations [29, 30]. In the well-structured microcolony biofilms, differentiation into subpopulations with different levels of the curli matrix production is largely deterministic and driven by gradients of nutrients and oxygen [18]. Bimodality of curli expression might also emerge stochastically, in a well-mixed population or between cells within the same layer of the macrocolony [27, 29, 30]. How this bimodality originates within the extremely complex regulatory network of curli genes [17, 19, 23, 27] remains a matter of debate. Although earlier studies in *S.* Typhimurium proposed that bistable expression of curli might be a consequence of positive transcriptional feedback in *csgD* regulation [29, 30, 41], the most recently proposed model attributed bistability to the properties of the c-di-GMP regulatory switch formed by DgcM, PdeR and MlrA [27, 31]. Furthermore, the dynamics of curli gene expression in individual cells remains unstudied.

Here, we investigated the bimodal expression of the major curli *csgBAC* operon at the population level in the well-stirred planktonic *E. coli* culture as well as on the single-cell level in the microfluidic device. Consistent with previous studies [12, 14], the induction of curli expression in growing *E. coli* cell population was observed during the entry into the stationary

phase of growth. Curli activation was apparently dependent on depletion of the amino acids from the medium, since it could be suppressed by increasing the levels of nutrients or, specifically, of serine. It might thus be related to induction of the stringent response, and consistently, it was enhanced by the SHX-mediated stimulation of the stringent response.

We further observed that activation of the *csgBAC* operon was strongly bimodal under all tested conditions, even in absence of any nutrient or other gradients. Stochastic nature of this activation was confirmed by incubation of *E. coli* cells in the microfluidic device, where upon a shift to the conditioned medium only a fraction of the cell population turned on the curli expression. Such differentiation is apparently consistent with previous observations of the bimodal *csgD* expression in *S.* Typhimurium [29, 30] and in *E. coli* [27]. However, whether the bimodality of the *csgBAC* expression is caused by the bimodal expression of *csgD* remains clear, since the latter was reported only in the later stationary phase of the culture growth [27, 29, 30], whereas in our experiments the *csgBAC* reporter showed bimodality already at an earlier stage.

In contrast to those previous interpretations of the *csgD* expression pattern as bistability, our data suggest that curli activation is only transient, and therefore bimodal but not bistable. Under conditions of continuous cell growth in the microfluidic device, the activation of curli expression is followed by its inactivation, indicating a pulsatile activation of the curli-positive state. Pulsing in expression was proposed to be common to many gene regulatory circuits [42], although only few well-studied examples such as stress response and differentiation in *Bacillus subtilis* [43, 44] are available. Pulsatile expression has also been recently described in *E. coli* for the upstream regulator of curli, RpoS [45], as well as for the flagellar regulon [46, 47] that is anti-regulated with curli [28]. However, in neither of these cases did pulsing lead to apparent bimodality of expression, and their relation to the observed pulses in curli expression thus remains to be seen.

How does such stochastic pulsing of curli expression observed at the single-cell level lead to the differentiation into two very distinct subpopulations in the batch planktonic culture? This could be likely explained by the timing of curli activation, and by the duration of these observed expression pulses: Since the curli expression is only turned-on during transition to the stationary phase, individual cells can stochastically activate curli genes just before the culture growth ceases. In contrast to the continuous culture, subsequent reversion to the curli-negative state by inactivation and dilution by cell division is no longer possible in the stationary batch culture, and these initially curli-expressing cells will thus remain positive.

Importantly, the regulation by c-di-GMP is not required for the bimodal curli expression in *E. coli*, since the differentiation into distinct subpopulations still occurred when the control of CsgD expression by c-di-GMP was abolished, as observed both in the planktonic cultures and in the microfluidic device. The level of *csgBAC* expression in curli-positive cells was also little

affected by the c-di-GMP control. Nevertheless, this control is important during the establishment of bimodality: Firstly, global levels of c-di-GMP determine the fraction of curli-positive cells, via regulation of MlrA activity, which is respectively inhibited by PdeR when c-di-GMP is low and activated by DgcM at high c-di-GMP [22, 23]. Secondly, the c-di-GMP-dependent control affects the dynamics of curli gene pulsing, with the faster but more heterogeneous activation of curli expression in the absence of the c-di-GMP control. Thirdly, and possibly related to the previous observation, this control might also ensure that the fraction of curli-positive cells is less variable dependent on the growth conditions of *E. coli* population. Thus, our study reveals a novel regulatory function exhibited by the second messenger c-di-GMP, in stabilizing the bimodal gene expression.

Acknowledgements

We thank Sarah Hoch, Silvia González Sierra and Gabriele Malengo for technical help and advice.

References

1. Arnqvist A, Olsen A, Pfeifer J, Russell DG, Normark S. The Crl protein activates cryptic genes for curli formation and fibronectin binding in *Escherichia coli* HB101. Mol Microbiol. 1992;6(17):2443-52. Epub 1992/09/01. doi: 10.1111/j.1365-2958.1992.tb01420.x. PubMed PMID: 1357528.

2. Hufnagel DA, Depas WH, Chapman MR. The Biology of the *Escherichia coli* Extracellular Matrix. Microbiol Spectr. 2015;3(3). Epub 2015/07/18. doi: 10.1128/microbiolspec.MB-0014-2014. PubMed PMID: 26185090; PubMed Central PMCID: PMCPMC4507285.

3. Larsen P, Nielsen JL, Dueholm MS, Wetzel R, Otzen D, Nielsen PH. Amyloid adhesins are abundant in natural biofilms. Environmental Microbiology. 2007. doi: 10.1111/j.1462-2920.2007.01418.x.

4. Romling U, Bian Z, Hammar M, Sierralta WD, Normark S. Curli fibers are highly conserved between *Salmonella typhimurium* and *Escherichia coli* with respect to operon structure and regulation. J Bacteriol. 1998;180(3):722-31. Epub 1998/02/11. doi: 10.1128/JB.180.3.722-731.1998. PubMed PMID: 9457880; PubMed Central PMCID: PMCPMC106944.

5. Vidal O, Longin R, Prigent-Combaret C, Dorel C, Hooreman M, Lejeune P. Isolation of an *Escherichia coli* K-12 mutant strain able to form biofilms on inert surfaces: involvement of a new ompR allele that increases curli expression. J Bacteriol. 1998;180(9):2442-9. Epub 1998/05/09. doi: 10.1128/JB.180.9.2442-2449.1998. PubMed PMID: 9573197; PubMed Central PMCID: PMCPMC107187.

6. Zogaj X, Bokranz W, Nimtz M, Romling U. Production of cellulose and curli fimbriae by members of the family Enterobacteriaceae isolated from the human gastrointestinal tract. Infect Immun. 2003;71(7):4151-8. Epub 2003/06/24. doi: 10.1128/IAI.71.7.4151-4158.2003. PubMed PMID: 12819107; PubMed Central PMCID: PMCPMC162016.

7. Tursi SA, Tukel C. Curli-Containing Enteric Biofilms Inside and Out: Matrix Composition, Immune Recognition, and Disease Implications. Microbiol Mol Biol Rev. 2018;82(4). Epub 2018/10/12. doi: 10.1128/MMBR.00028-18. PubMed PMID: 30305312; PubMed Central PMCID: PMCPMC6298610.
8. Chapman MR, Robinson LS, Pinkner JS, Roth R, Heuser J, Hammar M, et al. Role of *Escherichia coli* curli operons in directing amyloid fiber formation. Science. 2002;295(5556):851-5. Epub 2002/02/02. doi: 10.1126/science.1067484. PubMed PMID: 11823641; PubMed Central PMCID: PMCPMC2838482.
9. Dueholm MS, Albertsen M, Otzen D, Nielsen PH. Curli Functional Amyloid Systems Are Phylogenetically Widespread and Display Large Diversity in Operon and Protein Structure. PLoS ONE. 2012. doi: 10.1371/journal.pone.0051274.
10. Gerstel U, Römling U. The csgD promoter, a control unit for biofilm formation in *Salmonella typhimurium*. Research in Microbiology2003.
11. Brombacher E, Baratto A, Dorel C, Landini P. Gene expression regulation by the Curli activator CsgD protein: modulation of cellulose biosynthesis and control of negative determinants for microbial adhesion. J Bacteriol. 2006;188(6):2027-37. Epub 2006/03/04. doi: 10.1128/JB.188.6.2027-2037.2006. PubMed PMID: 16513732; PubMed Central PMCID: PMCPMC1428138.
12. Pesavento C, Becker G, Sommerfeldt N, Possling A, Tschowri N, Mehlis A, et al. Inverse regulatory coordination of motility and curli-mediated adhesion in *Escherichia coli*. Genes Dev. 2008;22(17):2434-46. Epub 2008/09/04. doi: 10.1101/gad.475808. PubMed PMID: 18765794; PubMed Central PMCID: PMCPMC2532929.
13. Romling U, Rohde M, Olsen A, Normark S, Reinkoster J. AgfD, the checkpoint of multicellular and aggregative behaviour in *Salmonella typhimurium* regulates at least two independent pathways. Mol Microbiol. 2000;36(1):10-23. Epub 2000/04/12. doi: 10.1046/j.1365-2958.2000.01822.x. PubMed PMID: 10760159.
14. Weber H, Pesavento C, Possling A, Tischendorf G, Hengge R. Cyclic-di-GMP-mediated signalling within the sigma network of *Escherichia coli*. Mol Microbiol. 2006;62(4):1014-34. Epub 2006/10/03. doi: 10.1111/j.1365-2958.2006.05440.x. PubMed PMID: 17010156.
15. Barnhart MM, Chapman MR. Curli biogenesis and function. Annu Rev Microbiol. 2006;60:131-47. Epub 2006/05/18. doi: 10.1146/annurev.micro.60.080805.142106. PubMed PMID: 16704339; PubMed Central PMCID: PMCPMC2838481.
16. Ishihama A. Prokaryotic genome regulation: Multifactor promoters, multitarget regulators and hierarchic networks. FEMS Microbiology Reviews2010.
17. Rossi E, Cimdins A, Luthje P, Brauner A, Sjoling A, Landini P, et al. "It's a gut feeling" - *Escherichia coli* biofilm formation in the gastrointestinal tract environment. Crit Rev Microbiol. 2018;44(1):1-30. Epub 2017/05/10. doi: 10.1080/1040841X.2017.1303660. PubMed PMID: 28485690.
18. Serra DO, Hengge R. Bacterial Multicellularity: The Biology of *Escherichia coli* Building Large-Scale Biofilm Communities. Annu Rev Microbiol. 2021;75:269-90. Epub 2021/08/04. doi: 10.1146/annurev-micro-031921-055801. PubMed PMID: 34343018.
19. Simm R, Ahmad I, Rhen M, Le Guyon S, Romling U. Regulation of biofilm formation in *Salmonella enterica* serovar Typhimurium. Future Microbiol. 2014;9(11):1261-82. Epub 2014/12/02. doi: 10.2217/fmb.14.88. PubMed PMID: 25437188.
20. Brown PK, Dozois CM, Nickerson CA, Zuppardo A, Terlonge J, Curtiss R. MIrA, a novel regulator of curli (AgF) and extracellular matrix synthesis by *Escherichia coli* and *Salmonella*

414 *enterica* serovar Typhimurium. Molecular Microbiology. 2001. doi: 10.1046/j.1365-
415 2958.2001.02529.x.
416 21. Ogasawara H, Yamada K, Kori A, Yamamoto K, Ishihama A. Regulation of the
417 *Escherichia coli* csgD promoter: Interplay between five transcription factors. Microbiology.
418 2010. doi: 10.1099/mic.0.039131-0.
419 22. Lindenberg S, Klauck G, Pesavento C, Klauck E, Hengge R. The EAL domain protein YciR
420 acts as a trigger enzyme in a c-di-GMP signalling cascade in *E. coli* biofilm control. EMBO J.
421 2013;32(14):2001-14. Epub 2013/05/28. doi: 10.1038/emboj.2013.120. PubMed PMID:
422 23708798; PubMed Central PMCID: PMCPMC3715855.
423 23. Hengge R. Linking bacterial growth, survival, and multicellularity - small signaling
424 molecules as triggers and drivers. Curr Opin Microbiol. 2020;55:57-66. Epub 2020/04/04. doi:
425 10.1016/j.mib.2020.02.007. PubMed PMID: 32244175.
426 24. Sarenko O, Klauck G, Wilke FM, Pfiffer V, Richter AM, Herbst S, et al. More than
427 Enzymes That Make or Break Cyclic Di-GMP-Local Signaling in the Interactome of GGDEF/EAL
428 Domain Proteins of *Escherichia coli*. mBio. 2017;8(5). Epub 2017/10/12. doi:
429 10.1128/mBio.01639-17. PubMed PMID: 29018125; PubMed Central PMCID:
430 PMCPMC5635695.
431 25. DePas WH, Hufnagel DA, Lee JS, Blanco LP, Bernstein HC, Fisher ST, et al. Iron induces
432 bimodal population development by *Escherichia coli*. Proc Natl Acad Sci U S A.
433 2013;110(7):2629-34. Epub 2013/01/30. doi: 10.1073/pnas.1218703110. PubMed PMID:
434 23359678; PubMed Central PMCID: PMCPMC3574911.
435 26. Serra DO, Richter AM, Klauck G, Mika F, Hengge R. Microanatomy at cellular resolution
436 and spatial order of physiological differentiation in a bacterial biofilm. mBio.
437 2013;4(2):e00103-13. Epub 2013/03/21. doi: 10.1128/mBio.00103-13. PubMed PMID:
438 23512962; PubMed Central PMCID: PMCPMC3604763.
439 27. Serra DO, Hengge R. A c-di-GMP-Based Switch Controls Local Heterogeneity of
440 Extracellular Matrix Synthesis which Is Crucial for Integrity and Morphogenesis of *Escherichia*
441 *coli* Macrocolony Biofilms. J Mol Biol. 2019;431(23):4775-93. Epub 2019/04/08. doi:
442 10.1016/j.jmb.2019.04.001. PubMed PMID: 30954572.
443 28. Besharova O, Suchanek VM, Hartmann R, Drescher K, Sourjik V. Diversification of gene
444 expression during formation of static submerged biofilms by *Escherichia coli*. Frontiers in
445 Microbiology. 2016. doi: 10.3389/fmicb.2016.01568.
446 29. Grantcharova N, Peters V, Monteiro C, Zakikhany K, Römling U. Bistable expression of
447 CsgD in biofilm development of *Salmonella enterica* serovar Typhimurium. Journal of
448 Bacteriology. 2010. doi: 10.1128/JB.01826-08.
449 30. MacKenzie KD, Wang Y, Shivak DJ, Wong CS, Hoffman LJ, Lam S, et al. Bistable
450 expression of CsgD in *Salmonella enterica* serovar Typhimurium connects virulence to
451 persistence. Infect Immun. 2015;83(6):2312-26. Epub 2015/04/01. doi: 10.1128/IAI.00137-15.
452 PubMed PMID: 25824832; PubMed Central PMCID: PMCPMC4432751.
453 31. Yousef KP, Streck A, Schütte C, Siebert H, Hengge R, von Kleist M. Logical-continuous
454 modelling of post-translationally regulated bistability of curli fiber expression in *Escherichia*
455 *coli*. BMC Systems Biology. 2015. doi: 10.1186/s12918-015-0183-x.
456 32. Baba T, Ara T, Hasegawa M, Takai Y, Okumura Y, Baba M, et al. Construction of
457 *Escherichia coli* K-12 in-frame, single-gene knockout mutants: the Keio collection. Mol Syst
458 Biol. 2006;2:2006 0008. Epub 2006/06/02. doi: 10.1038/msb4100050. PubMed PMID:
459 16738554; PubMed Central PMCID: PMCPMC1681482.

460 33. Cherepanov PP, Wackernagel W. Gene disruption in *Escherichia coli*: TcR and KmR
461 cassettes with the option of Flp-catalyzed excision of the antibiotic-resistance determinant.
462 Gene. 1995;158(1):9-14. Epub 1995/05/26. doi: 10.1016/0378-1119(95)00193-a. PubMed
463 PMID: 7789817.
464 34. Amann E, Ochs B, Abel K-J. Tightly regulated tac promoter vectors useful for the
465 expression of unfused and fused proteins in *Escherichia coli*. Gene. 1988;69(2):301-15. doi:
466 https://doi.org/10.1016/0378-1119(88)90440-4.
467 35. Wang P, Robert L, Pelletier J, Dang WL, Taddei F, Wright A, et al. Robust growth of
468 *Escherichia coli*. Curr Biol. 2010;20(12):1099-103. Epub 2010/06/12. doi:
469 10.1016/j.cub.2010.04.045. PubMed PMID: 20537537; PubMed Central PMCID:
470 PMCPMC2902570.
471 36. Potrykus K, Cashel M. (p)ppGpp: still magical? Annu Rev Microbiol. 2008;62:35-51.
472 Epub 2008/05/06. doi: 10.1146/annurev.micro.62.081307.162903. PubMed PMID: 18454629.
473 37. Varik V, Oliveira SRA, Hauryliuk V, Tenson T. HPLC-based quantification of bacterial
474 housekeeping nucleotides and alarmone messengers ppGpp and pppGpp. Sci Rep.
475 2017;7(1):11022. Epub 2017/09/10. doi: 10.1038/s41598-017-10988-6. PubMed PMID:
476 28887466; PubMed Central PMCID: PMCPMC5591245.
477 38. Patacq C, Chaudet N, Letisse F. Crucial Role of ppGpp in the Resilience of *Escherichia*
478 *coli* to Growth Disruption. mSphere. 2020;5(6). Epub 2020/12/29. doi:
479 10.1128/mSphere.01132-20. PubMed PMID: 33361126; PubMed Central PMCID:
480 PMCPMC7763551.
481 39. Krasteva PV, Fong JC, Shikuma NJ, Beyhan S, Navarro MV, Yildiz FH, et al. *Vibrio*
482 *cholerae* VpsT regulates matrix production and motility by directly sensing cyclic di-GMP.
483 Science. 2010;327(5967):866-8. Epub 2010/02/13. doi: 10.1126/science.1181185. PubMed
484 PMID: 20150502; PubMed Central PMCID: PMCPMC2828054.
485 40. Ahmad I, Cimdins A, Beske T, Romling U. Detailed analysis of c-di-GMP mediated
486 regulation of csgD expression in *Salmonella typhimurium*. BMC Microbiol. 2017;17(1):27. Epub
487 2017/02/06. doi: 10.1186/s12866-017-0934-5. PubMed PMID: 28148244; PubMed Central
488 PMCID: PMCPMC5289004.
489 41. Gualdi L, Tagliabue L, Landini P. Biofilm formation-gene expression relay system in
490 *Escherichia coli*: modulation of sigmaS-dependent gene expression by the CsgD regulatory
491 protein via sigmaS protein stabilization. J Bacteriol. 2007;189(22):8034-43. Epub 2007/09/18.
492 doi: 10.1128/JB.00900-07. PubMed PMID: 17873038; PubMed Central PMCID:
493 PMCPMC2168689.
494 42. Levine JH, Lin Y, Elowitz MB. Functional roles of pulsing in genetic circuits. Science.
495 2013;342(6163):1193-200. Epub 2013/12/07. doi: 10.1126/science.1239999. PubMed PMID:
496 24311681; PubMed Central PMCID: PMCPMC4100686.
497 43. Locke JC, Young JW, Fontes M, Hernandez Jimenez MJ, Elowitz MB. Stochastic pulse
498 regulation in bacterial stress response. Science. 2011;334(6054):366-9. Epub 2011/10/08. doi:
499 10.1126/science.1208144. PubMed PMID: 21979936; PubMed Central PMCID:
500 PMCPMC4100694.
501 44. Levine JH, Fontes ME, Dworkin J, Elowitz MB. Pulsed feedback defers cellular
502 differentiation. PLoS Biol. 2012;10(1):e1001252. Epub 2012/02/04. doi:
503 10.1371/journal.pbio.1001252. PubMed PMID: 22303282; PubMed Central PMCID:
504 PMCPMC3269414.
505 45. Patange O, Schwall C, Jones M, Villava C, Griffith DA, Phillips A, et al. *Escherichia coli*
506 can survive stress by noisy growth modulation. Nat Commun. 2018;9(1):5333. Epub

2018/12/19. doi: 10.1038/s41467-018-07702-z. PubMed PMID: 30559445; PubMed Central PMCID: PMCPMC6297224.

46. Kim JM, Garcia-Alcala M, Balleza E, Cluzel P. Stochastic transcriptional pulses orchestrate flagellar biosynthesis in *Escherichia coli*. Sci Adv. 2020;6(6):eaax0947. Epub 2020/02/23. doi: 10.1126/sciadv.aax0947. PubMed PMID: 32076637; PubMed Central PMCID: PMCPMC7002133.

47. Sassi AS, Garcia-Alcala M, Kim MJ, Cluzel P, Tu Y. Filtering input fluctuations in intensity and in time underlies stochastic transcriptional pulses without feedback. Proc Natl Acad Sci U S A. 2020;117(43):26608-15. Epub 2020/10/14. doi: 10.1073/pnas.2010849117. PubMed PMID: 33046652; PubMed Central PMCID: PMCPMC7604450.

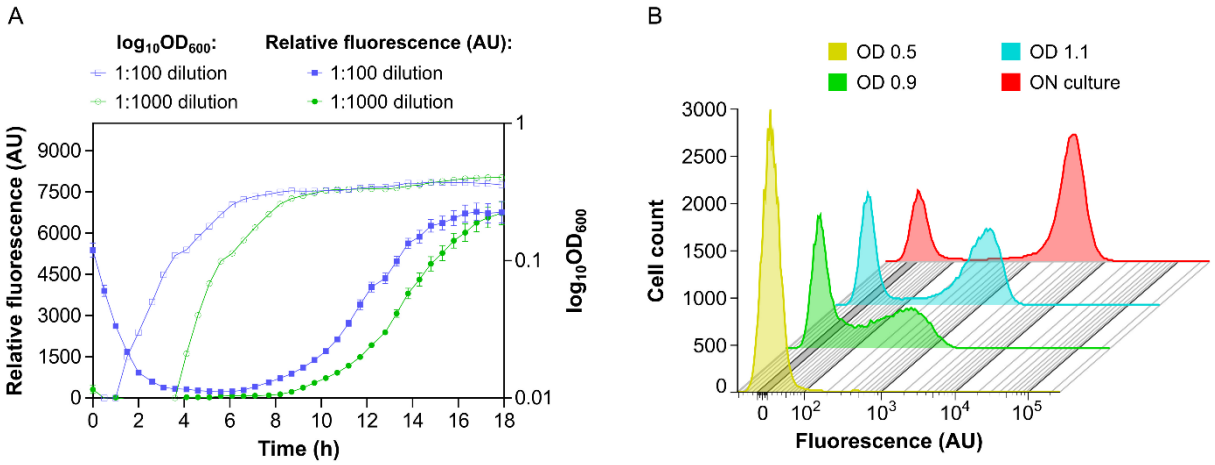

Figure 1: Bimodal activation of curli gene expression in *E. coli* planktonic cultures. *E. coli* cells carrying genomic transcriptional reporter of *csgBAC* operon were grown in liquid tryptone broth (TB) medium at 30 °C under constant shaking. **(A)** Optical density (OD_{600}) and relative fluorescence (fluorescence/OD_{600}; AU, arbitrary units) of the culture during growth in a plate reader, starting from two different dilutions of the overnight culture. Error bars indicate standard error of the mean (SEM) of 10 technical replicates. **(B)** Distribution of single-cell fluorescence levels in cultures grown to indicated OD_{600} or overnight (ON; 25 h) in an orbital shaker, measured by flow cytometry.

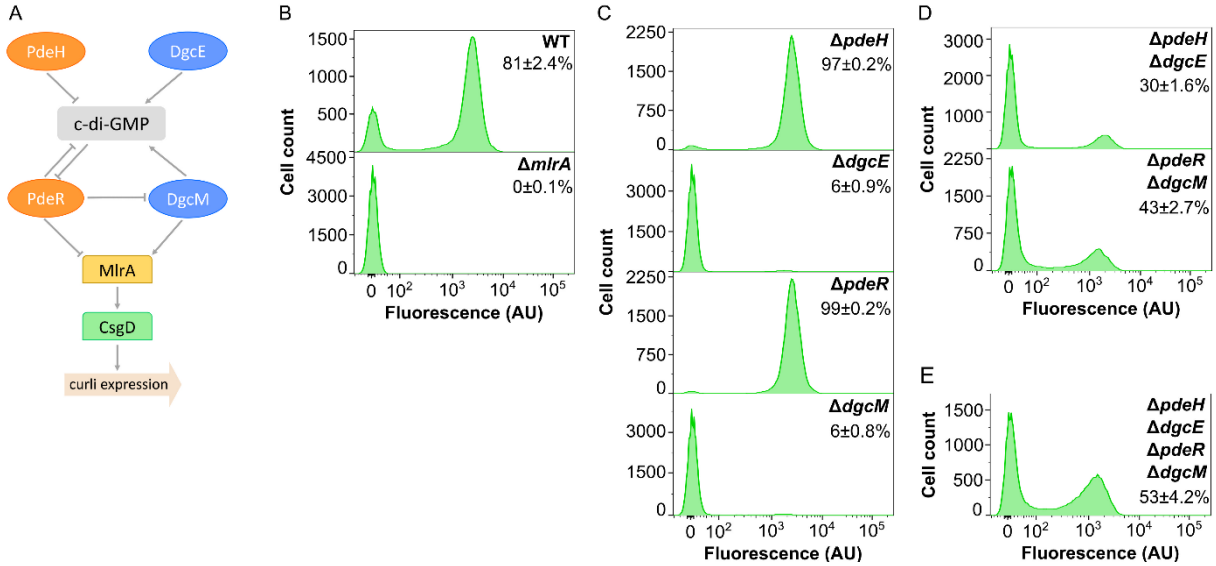

Figure 2: Regulation of curli expression by c-di-GMP. (A) Current model of regulation of curli gene expression by c-di-GMP in *E. coli*, adapted from [27]. The regulation is mediated by two pairs of diguanylate cyclases (DGCs; blue) and phosphodiestherases (PDEs; orange). PdeH and DgcE control global level of c-di-GMP, whereas PdeR and DgcM mediate local c-di-GMP-dependent regulation of curli gene expression by controlling activity of transcription factor MlrA, which activates another curli-specific transcription factor CsgD. **(B-E)** Flow cytometry measurements of curli gene expression in *E. coli* planktonic cultures grown overnight in flasks in an orbital shaker, shown for the wildtype (WT) and Δ*mlrA* knockout (B), and individual (C), double (D) and quadruple (E) knockouts of DGC or PDE enzymes, as indicated. Fraction of positive cells in the population (mean of three biological replicates ± SEM) is indicated for each strain. Note that the scale in the *y* axes is different for individual strains to improve readability.

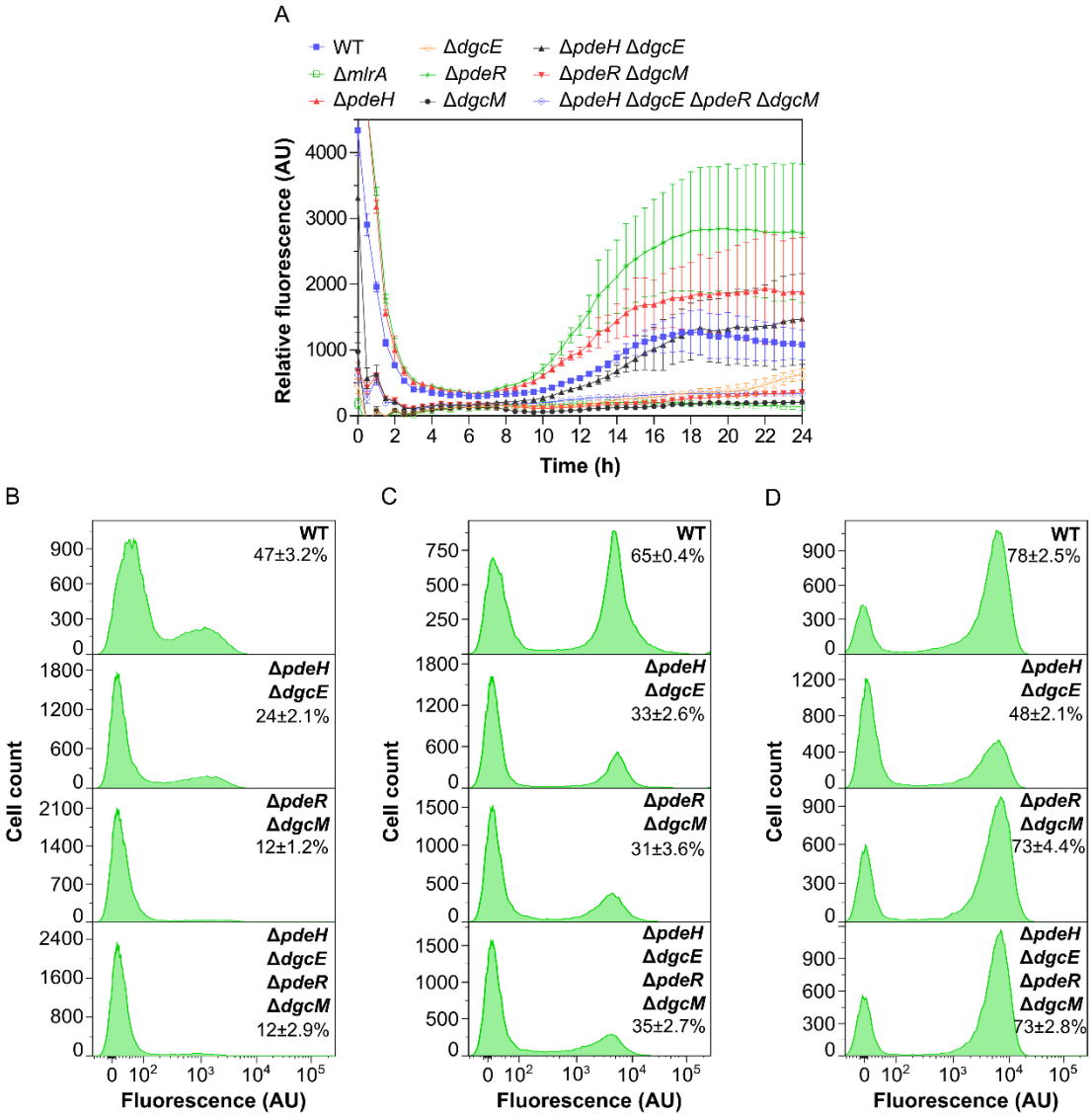

Figure 3: Dependence of curli expression on c-di-GMP regulation under different growth conditions. (A) Relative fluorescence of transcriptional curli reporter in planktonic culture grown in a plate reader. Error bars indicate SEM of 5 technical replicates. **(B-D)** Flow cytometry measurements of curli expression in the wildtype (WT) and indicated knockout strains after 24 h of growth either in a plate reader (B), as submerged biofilms (C) or as macrocolony biofilms (D). Measurements for other knock-outs are shown in Figures S4, S6A, S7A. Fraction of positive cells in the population (mean of three biological replicates ± SEM) is indicated for each strain. Note that the scale in the *y* axes is different for individual strains to improve readability.

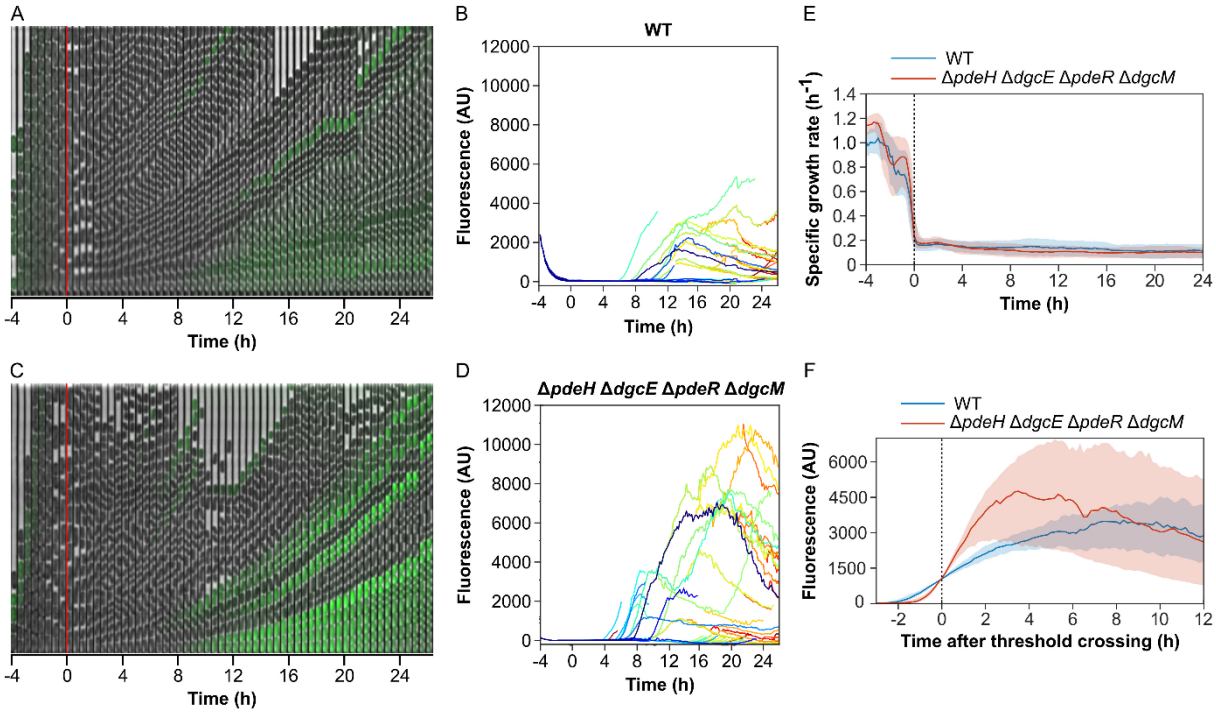

Figure 4: Impact of c-di-GMP regulation on dynamics of curli induction in individual cells. *E. coli* cells in a microfluidic device (mother machine) were shifted from a fresh to conditioned TB medium after 4 h of growth to induce curli expression. **(A-D)** Examples of image time series and single-cell fluorescence traces for the wildtype (WT) (A,B) and for the Δ*pdeH* Δ*dgcE* Δ*pdeR* Δ*dgcM* strain disabled in the c-di-GMP regulation (C,D) growing in a mother machine in one experiment. Expression of the curli reporter is indicated by the green overlay on the phase contrast image. **(E)** Median instantaneous growth rate — fold rate of change in length — of cells grown in microfluidics experiments as described in (A). The switch to conditioned medium is at time zero, as indicated. Shaded area is the interquartile range. The number of cells in the device varies with time, but is on average n = 296 for WT and n = 522 for the quadruple knockout. **(F)** Median curli expression profile for single-cell traces aligned by the time at which they exceed a threshold of 10^3 fluorescence units. Shaded area is interquartile range; n = 128 for WT and 230 for the quadruple knockout.

Supporting information

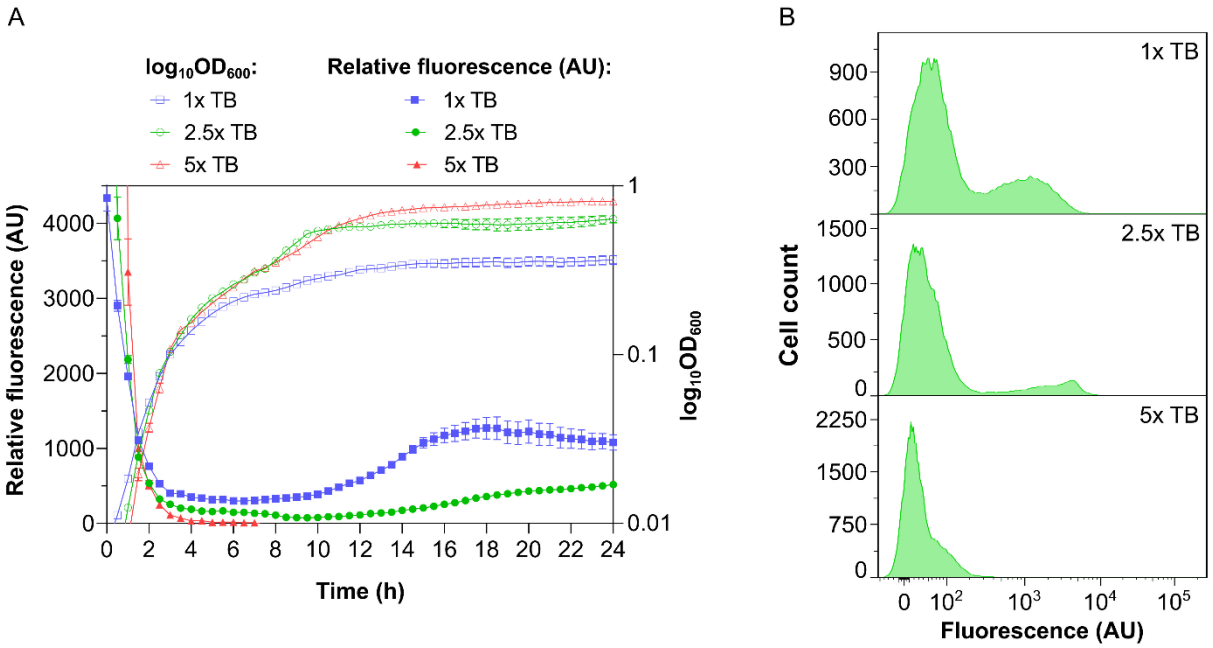

Figure S1: Dependence of curli gene expression on nutrient levels. Wildtype *E. coli* cultures were grown as in Figure 1A but with different indicated concentrations of TB. **(A)** Bacterial growth and activity of transcriptional curli reporter. Error bars indicate SEM of 6 technical replicates. **(B)** Distribution of single-cell fluorescence levels after 24 h of growth in a plate reader measured by flow cytometry. Note that the scale in the *y* axes is different for individual conditions to improve readability.

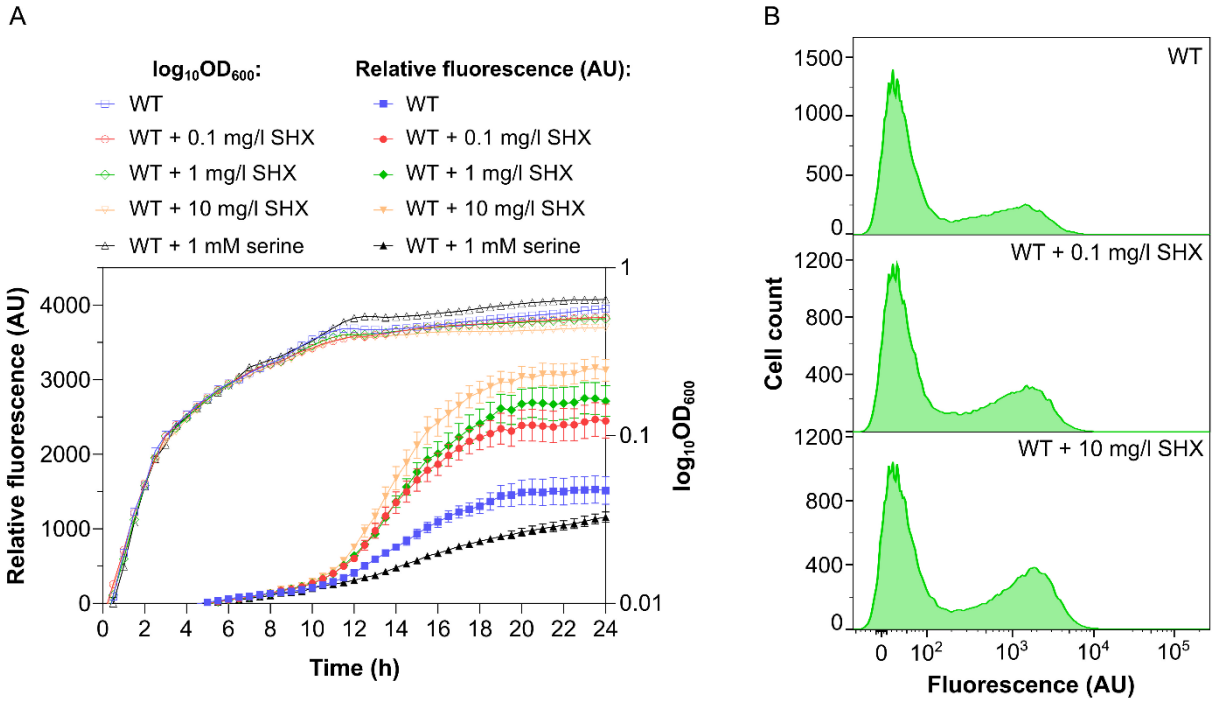

Figure S2: Stimulation of curli gene expression by stringent response. Wildtype *E. coli* cultures were grown as in Figure 1A but with addition of either indicated concentrations of serine hydroxamate (SHX) at inoculation point or 1 mM serine after 6 h of growth. **(A)** Bacterial growth and activity of transcriptional curli reporter. Error bars indicate SEM of 6 technical replicates. **(B)** Distribution of single-cell fluorescence levels after 24 h of growth in a plate reader measured by flow cytometry. Note that the scale in the *y* axes is different for individual conditions to improve readability.

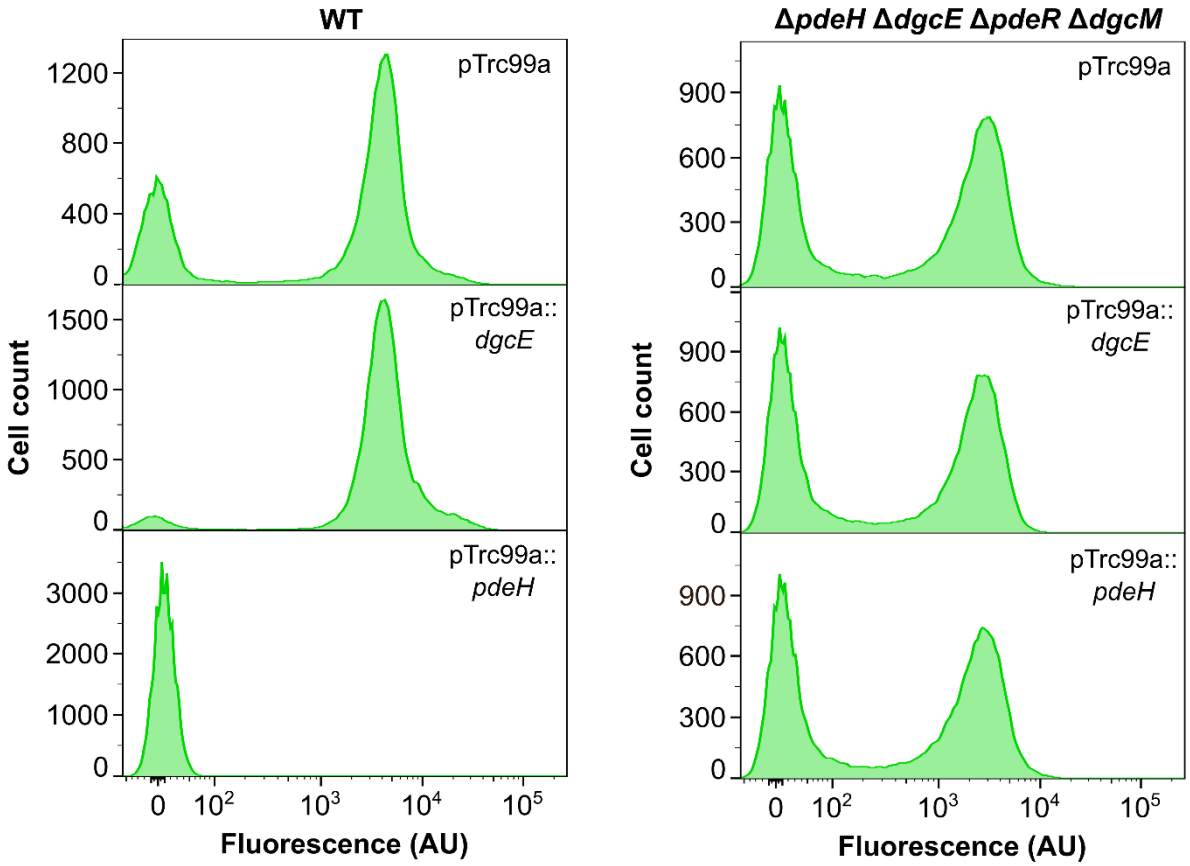

Figure S3: Decoupling of curli gene expression from c-di-GMP regulation in the absence of PdeR/ DgcM regulatory module. *E. coli* wildtype (WT) cells or cells lacking c-di-GMP regulatory enzymes (Δ*pdeH* Δ*dgcE* Δ*pdeR* Δ*dgcM*) were transformed with either empty pTrc99a plasmid (control) or with pTrc99a plasmid carrying *dgcE* (pTrc99a::dgcE) or *pdeH* (pTrc99a::pdeH) genes. Expression from the vector was induced with 1 μM IPTG. Bacteria were grown overnight in flasks with shaking and cultures were subjected to the flow cytometry analysis. Note that the scale in the *y* axes is different for individual strains to improve readability.

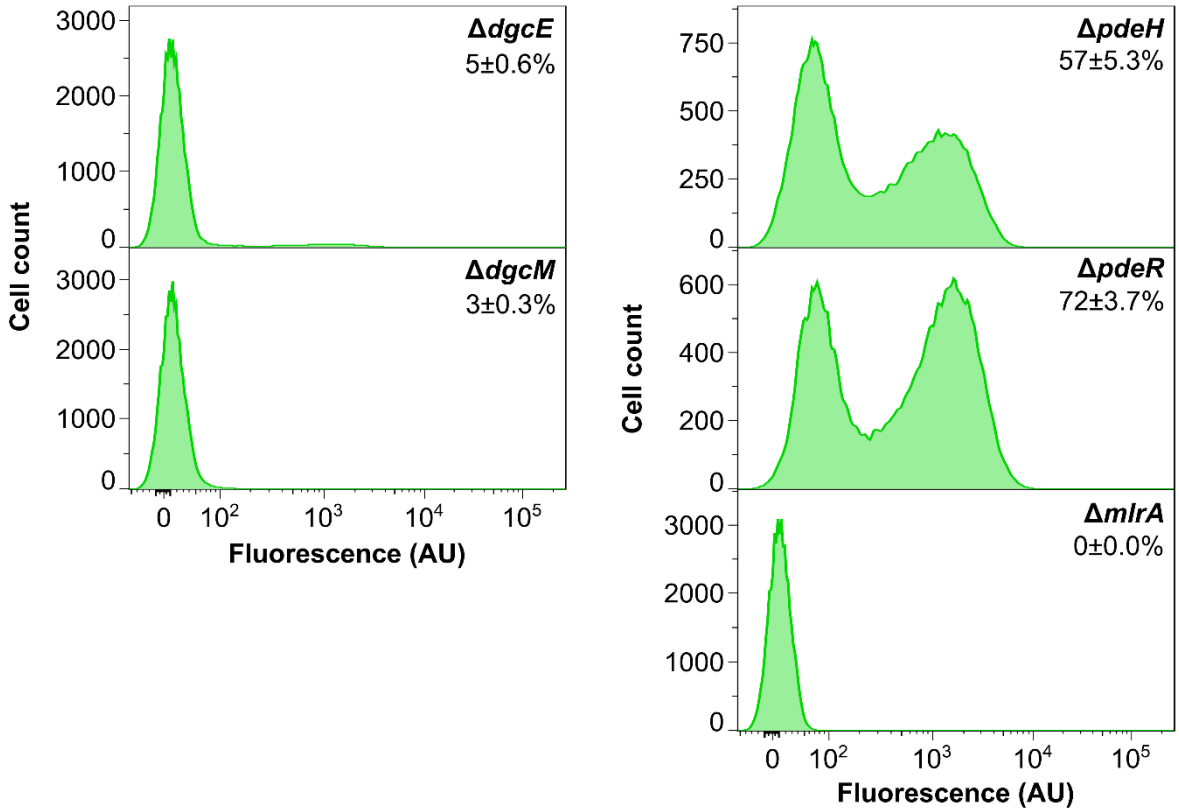

586

587 **Figure S4: Curli gene expression in cultures grown in a plate reader.** *E. coli* cells were grown as in
588 Figure 3A,B. Flow cytometry measurements for indicated knockouts are shown. Measurements in other
589 strains are shown in Figure 3B. Fraction of positive cells in the population (mean of three biological
590 replicates ± SEM) is indicated for each strain. Note that the scale in the *y* axes is different for individual
591 strains to improve readability.

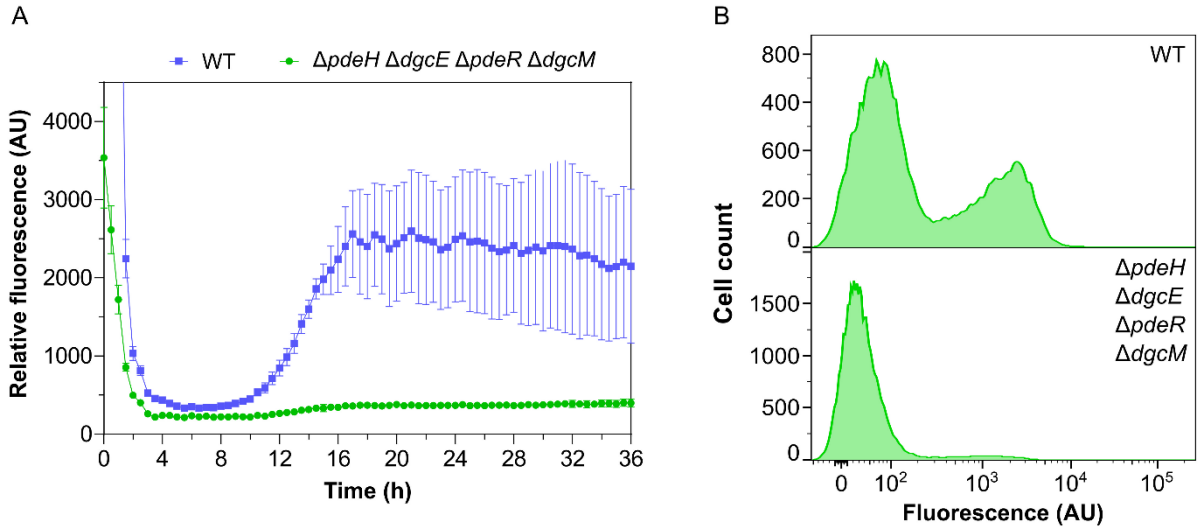

Figure S5: Curli gene expression upon prolonged cultivation in a plate reader. Wildtype (WT) and (Δ*pdeH* Δ*dgcE* Δ*pdeR* Δ*dgcM*) knockout strains were grown in a plate reader as in Figure 2 A,B, but for 36 h. **(A)** Induction of transcriptional curli reporter. Error bars indicate SEM of 10 technical replicates. **(B)** Distribution of single-cell fluorescence levels in populations of both strains after 36 h of growth measured by flow cytometry.

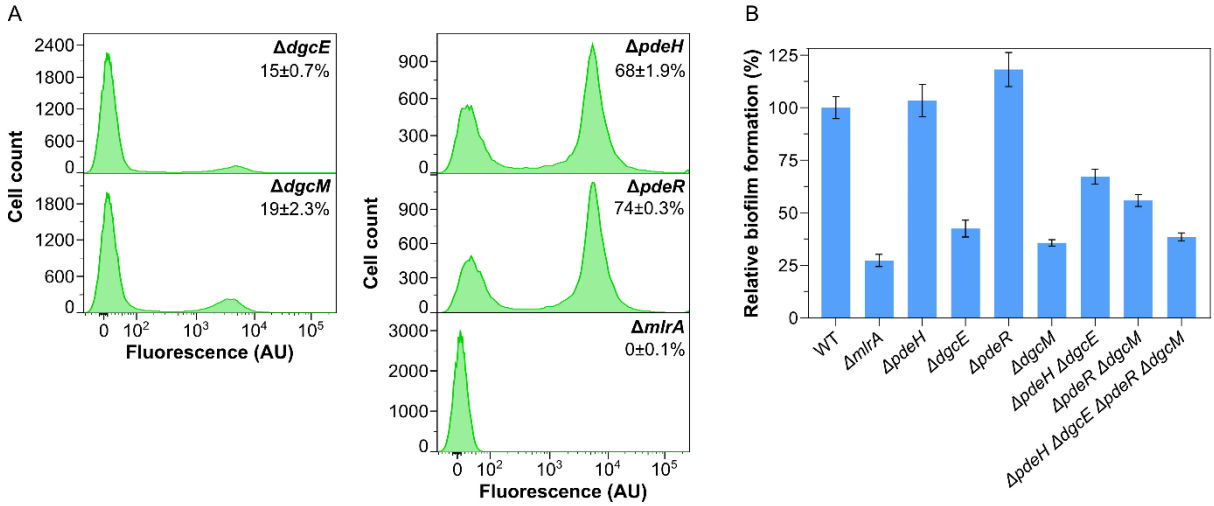

Figure S6: Curli gene expression in submerged biofilm cultures. (A) Distribution of single-cell fluorescence levels in populations of indicated knockout strains after 46 h of submerged biofilm culture growth, measured by flow cytometry. Measurements in other strains are shown in Figure 3C. Fraction of positive cells in the population (mean of three biological replicates ± SEM) is indicated for each strain. Note that the scale in the *y* axes is different for individual strains to improve readability. **(B)** Biofilm formation by indicated strains, quantified using crystal violet (CV) staining. Error bars indicate SEM of 3 independent replicates.

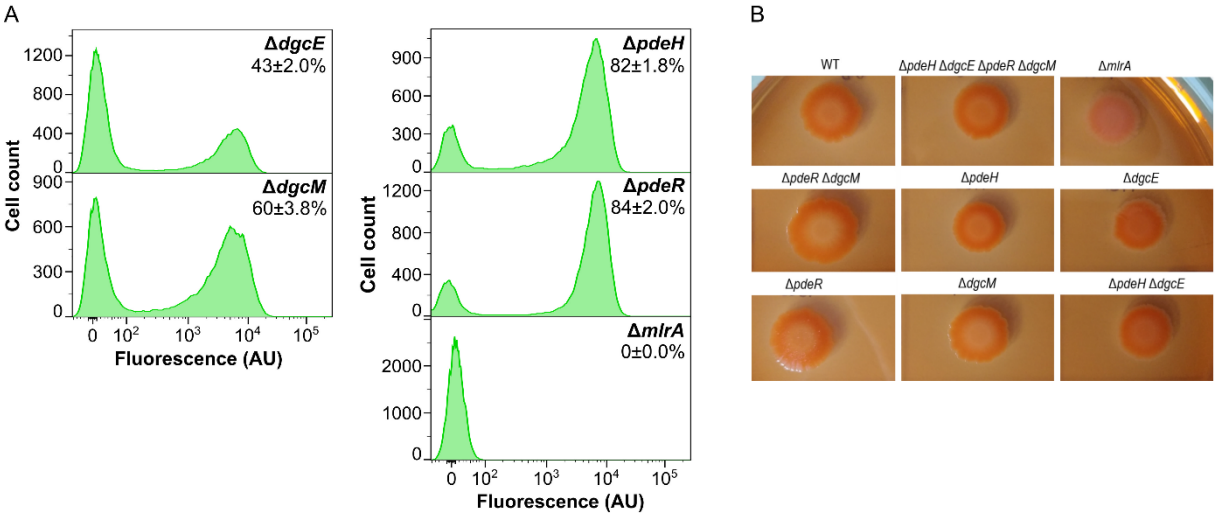

606

607 **Figure S7: Curli expression in macrocolony biofilms. (A,B)** Flow cytometry measurements of curli
608 expression (A) and images of microcolonies of indicated strains (B) after 8 days of growth. Flow
609 cytometry measurements for other strains are shown in Figure 3D. Fraction of positive cells in the
610 population (mean of three biological replicates ± SEM) is indicated for each strain. Note that the scale
611 in the *y* axes is different for individual strains to improve readability.

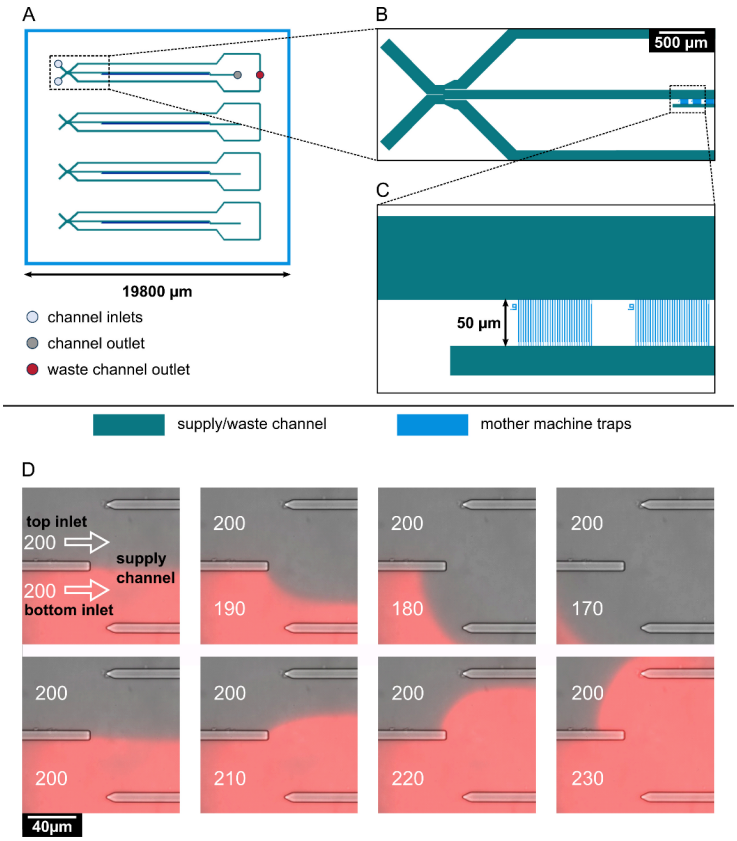

Figure S8: Design of the microfluidic mother machine chip. (A) Schematic overview on the channel layout, featuring four supply channels (green) for cell inoculation and media supply. **(B)** Detailed view of the area marked by a rectangle in (A), showing the switching junction and a part of the mother machine cultivation sites (blue). The junction is formed by two inlets, leading to one central supply channel. The control of the pressure at each inlet allows to choose the medium flowing through the supply channel, and, ultimately, to the mother machine cultivation sites. Residual medium flows out through the waste channels located on both sides from the central channel. Medium flowing through the supply channel exits the chip through one outlet. **(C)** Detailed view of the area marked in **(B)** by a rectangle, showing the mother machine cultivation sites. Each of the four channels contains 57 mother machine cultivation sites, which contain 30 mother machine traps with widths of 0.9, 1, or 1.1 µm. The mother machine traps feature a 0.3 µm wide constriction on the bottom, preventing the mother cell from exiting the trap while allowing medium perfusion. The supply channels (green) are 8 µm in depth, the mother machine traps (blue) are 0.8 µm in depth. **(D)** On-chip medium switching visualized by merged phase contrast and mCherry images of the channel junction. Media are supplied through separate inlets (top and bottom), which are separated in the center of the channel by a PDMS barrier. The direction of flow is indicated by white arrows. Water was supplied through the top inlet, while a 0.2 µM sulforhodamine B solution was supplied through the bottom inlet, visualizing the flow pattern in the junction. The pressure at the top inlet was kept constant at 200 mbar. Depending on the pressure set at the bottom inlet, it is possible to select which one of the two media flows into the central supply channel to the mother machine growth sites.

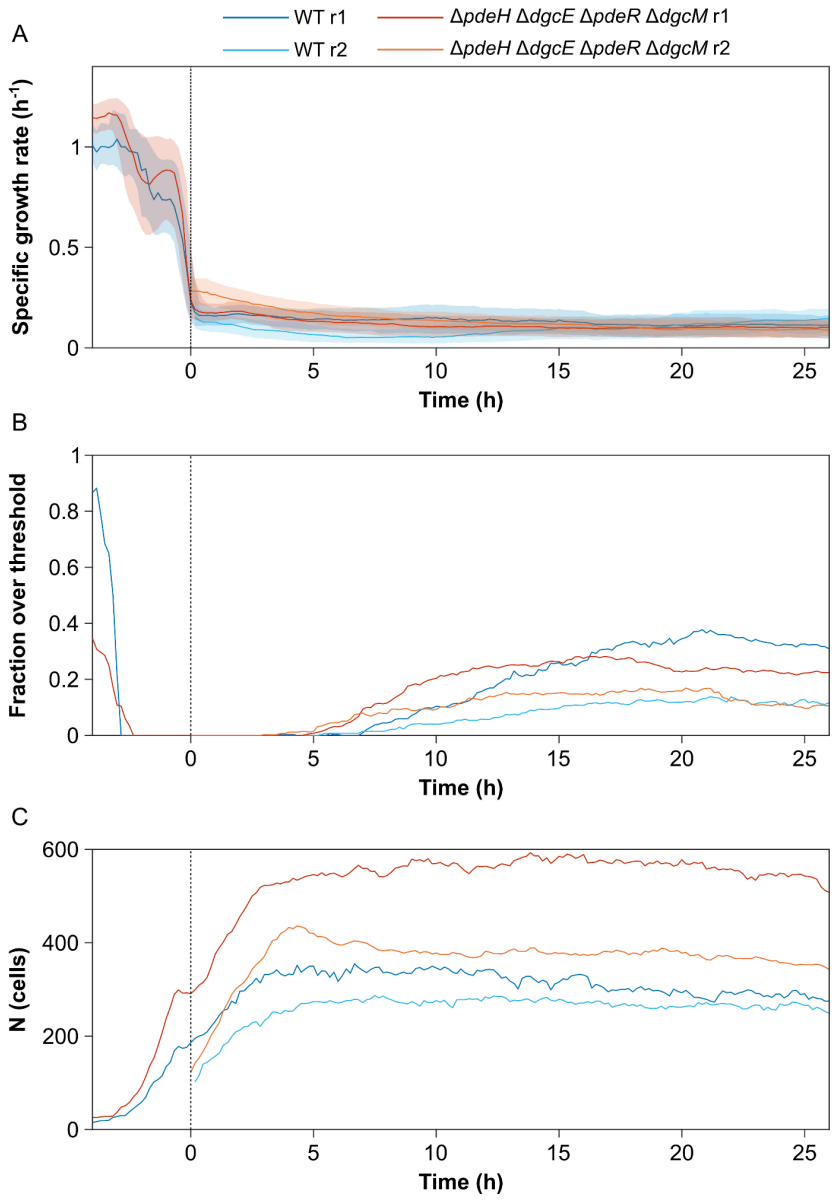

Figure S9: Growth rates and fraction of curli expressing cells over time. Stationary phase cells were introduced into mother machine devices, supplied with fresh medium and then switched to conditioned medium after four hours of growth, as in Figure 4. **(A)** Median instantaneous growth rates for the wildtype and for the Δ*pdeH* Δ*dgcE* Δ*pdeR* Δ*dgcM* strain disabled in the c-di-GMP regulation. Growth rate drops rapidly and cells switch on curli expression after a switch to conditioned medium. Shaded area is interquartile range. **(B)** Fraction of cells with fluorescence exceeding 1000 units. **(C)** Number of detected cells. Two biological replicates (r1 and r2) were performed for each strain; data for the r1 replicate are also shown in Figure 4. Note that in the experiment r2 cells were only imaged after medium switching.

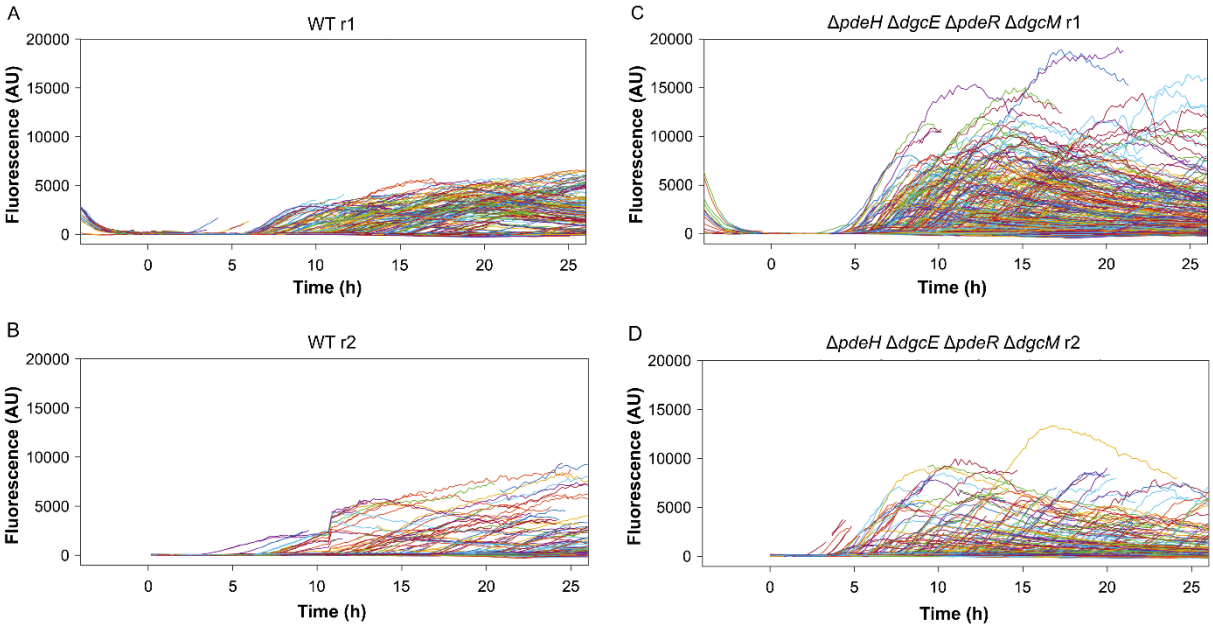

Figure S10: Single-cell traces of cell fluorescence for all cells for the wildtype and for the c-di-GMP-regulation disabled strain. Data are from the same biological replicates (r1 and r2) as in Figure S9.

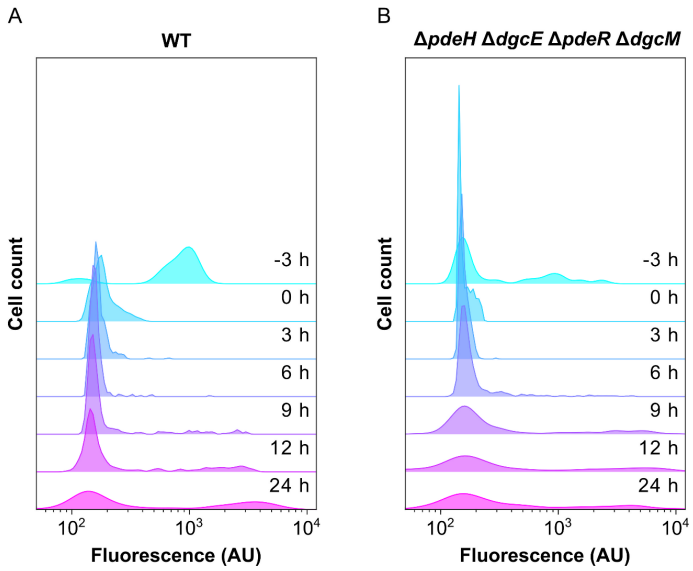

Figure S11: Distributions of curli expression at different time points in the microfluidics experiment. Shown are kernel density estimates of curli expression in the wildtype WT **(A)** and in the c-di-GMP-regulation disabled strain **(B)** at selected time points, for the replicate presented in Figure 4. In time order, for WT, n = 18, 158, 332, 317, 335, 342 and 285, and for the Δ*pdeH* Δ*dgcE* Δ*pdeR* Δ*dgcM* strain, n = 25, 247, 525, 546, 581, 546 and 544.

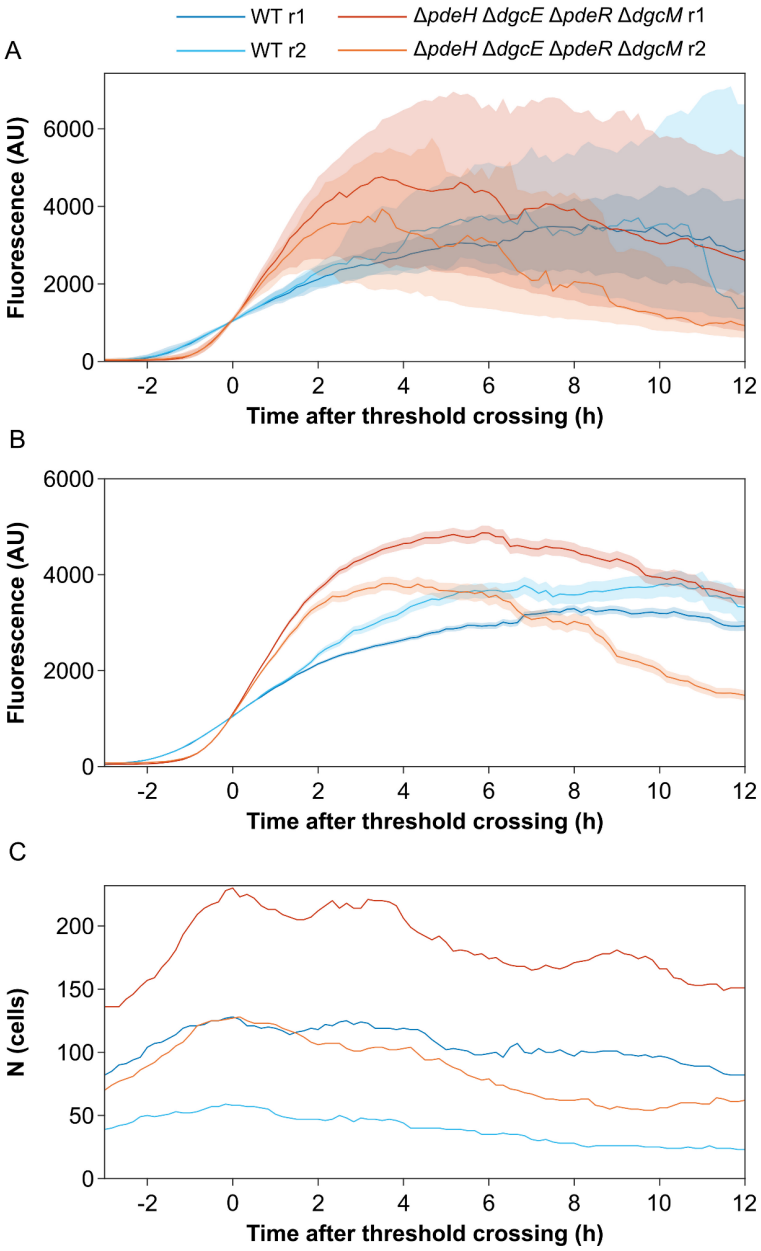

Figure S12: The rate and variability of curli induction for the wildtype and for the c-di-GMP-regulation disabled strain. (A) Median curli expression, **(B)** mean curli expression, **(C)** number of cells for traces from both microfluidics experiments (r1 and r2) aligned by the time at which they exceeded a threshold of 10^3 fluorescence units. Shaded area is interquartile range in (A) or standard error in (B). Compared to the WT, the rate of curli induction is faster but traces show more variability in a mutant without the global or local c-di-GMP regulatory modules.

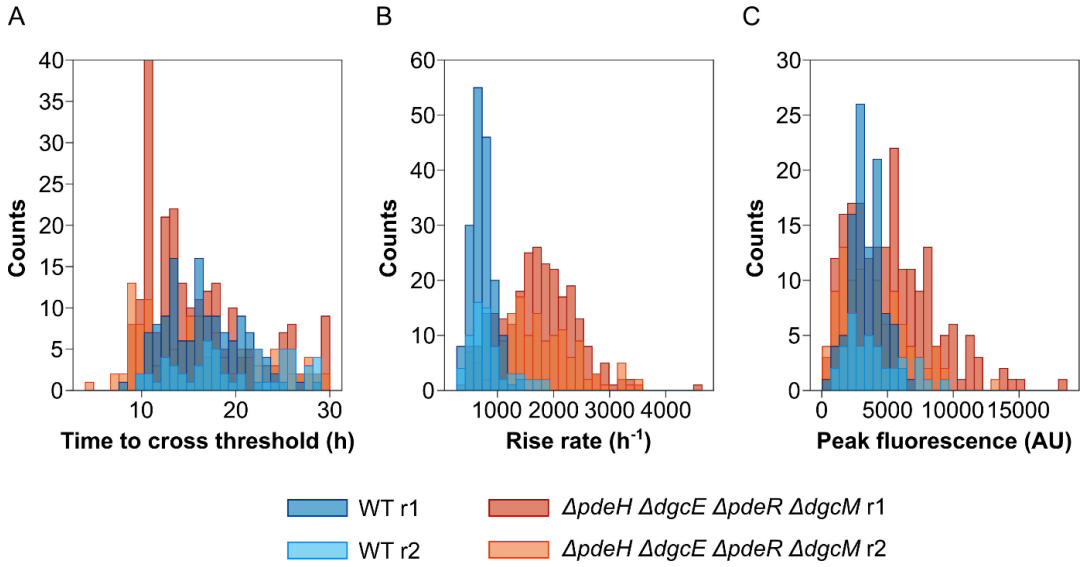

Figure S13: Distributions of curli induction parameters for the wildtype and for the c-di-GMP-regulation disabled strain. Shown are histograms of the times at which a threshold of 10^3 fluorescence units were crossed **(A)**, the maximum rates of increase in fluorescence **(B)**, or the fluorescence amplitudes at the first peak **(C)** for cell traces from both microfluidics experiments. Though switch timing is similar, rates of curli induction are faster and peak amplitudes more variable in a mutant without the global or local c-di-GMP regulatory modules.

668 **Table S1. *E. coli* strains and plasmids used in this study.**

Strains	Relevant genotype	Reference
W3110	W3110 derivative with functional RpoS	[1]
VS1146	W3110 *csgA*::*csgA*_RBS_*sfgfp*	[2]
VS1857	VS1146 Δ*mlrA*	This work
VS1732	VS1146 Δ*pdeH*	This work
VS1720	VS1146 Δ*dgcE*	This work
VS1258	VS1146 Δ*pdeR*	This work
VS1257	VS1146 Δ*dgcM*	This work
VS1717	VS1146 Δ*pdeH* Δ*dgcE*	This work
VS1713	VS1146 Δ*pdeR* Δ*dgcM*	This work
VS1729	VS1146 Δ*pdeH* Δ*dgcE* Δ*pdeR* Δ*dgcM*	This work
Plasmids		
pTrc99a	Expression vector; *Ptrc* promoter inducible by isopropyl-β-D-thiogalactopyranoside (IPTG); pBR ori; Ap^R	[3]
pVS2689	pTrc99a::*pdeH*	This work
pVS1644	pTrc99a::*dgcE*	This work

669

670 1. Serra DO, Richter AM, Klauck G, Mika F, Hengge R. Microanatomy at cellular resolution and
671 spatial order of physiological differentiation in a bacterial biofilm. mBio. 2013;4(2):e00103-13. Epub
672 2013/03/21. doi: 10.1128/mBio.00103-13. PubMed PMID: 23512962; PubMed Central PMCID:
673 PMCPMC3604763.
674 2. Besharova O, Suchanek VM, Hartmann R, Drescher K, Sourjik V. Diversification of gene
675 expression during formation of static submerged biofilms by *Escherichia coli*. Frontiers in Microbiology.
676 2016. doi: 10.3389/fmicb.2016.01568.
677 3. Amann E, Ochs B, Abel K-J. Tightly regulated tac promoter vectors useful for the expression of
678 unfused and fused proteins in *Escherichia coli*. Gene. 1988;69(2):301-15. doi:
679 https://doi.org/10.1016/0378-1119(88)90440-4.
680
681

Supporting protocols

Design and fabrication of the mother machine. A microfluidic device was used for time-resolved studies of *E. coli* growth and curli expression, which features mother machines traps for the observation of one-dimensional cell growth. The design of the microfluidic device is shown in Figure S8. The channel structure of the microfluidic device features four independent channels with a depth of 8 µm, allowing the realization of four conditions, e.g. different media compositions, in one experiment. Each channel contains two inlets enabling on-chip switching between two different media, which are supplied at defined pressures. By controlling the pressure ratio between the two inlets, the medium supplied at the higher pressure flows through the central channel following the junction, while the other medium is pushed away from the junction and flows out through the waste channel (Figure S8D). The medium which flows through the central channel reaches the mother machine cultivation sites before exiting the chip through a single outlet.

The device was produced using a two-layer soft lithography method as described previously[1]. Based on our in-house made design of the channel layout, a 100 mm silicon wafer was produced by e-beam lithography (ConScience, Sweden). The wafer contains the channel layout as a positive relief. The mother machine traps, which are shown in blue in Figure S8A-C, were structured by etching the wafer by 0.8 µm, giving the mother machine the appropriate vertical dimension for cell trapping. The supply channels, which are shown in green in Figure S8A-C, are implemented as photoresist structures with a height of 8 µm on the wafer. The wafer served as a master mold for liquid polydimethylsiloxane (Sylgard 184 PDMS, VwR International GmbH, Germany), which was mixed at volumetric ratio of 7:1 with a cross-linking agent, degassed in a desiccator for 30 minutes and poured over the wafer to a height of approximately 4 mm and thermally cured at 80 °C overnight. The cured PDMS was peeled off from the wafer and manually cut into separate chips. Inlet and outlet holes were punched with a 0.75 mm punching tool (Robbins True-Cut Disposable Biopsy Punch 0.75mm with Plunger, Robbins Instruments, USA). The surface of the chip was cleaned by a rinse with isopropanol and the application of adhesive tape (tesafilm, Germany) prior to bonding. The chip was irreversibly bonded to a glass substrate by applying oxygen plasma to both chip and glass surfaces (Diener Femto, Diener GmbH, Germany) and bringing the treated surfaces together. The bond was strengthened by storing the bonded device in the oven at 80 °C for two minutes. The device was mounted on an inverted fluorescence microscope (Nikon Eclipse Ti, Nikon Corporation, Japan) equipped with an incubator. The microscope setup included an Andor Zyla 4.2 sCMOS camera (Oxford Instruments, UK), an objective with 100x magnification (Plan Apochromat λ Oil, NA=1.45, WD=170 µm; Nikon, Japan) and a perfect focus system (Nikon Corporation, Japan) for focus drift compensation

719

720 **Growth experiments.** *E. coli* cells were allowed to grow in TB medium until the stationary
721 phase prior to inoculation into the device. Conditioned medium was prepared by cultivating the
722 wildtype *E. coli* cells in TB medium for 20 hours, after which the cell suspension was
723 centrifuged at 4000 rpm for ten minutes, the medium was filter sterilized and stored at 4°C.
724 The mother machine growth sites were loaded with the undiluted cell suspension by manual
725 infusion of the cell suspension through one of the two inlets using a 1-ml syringe. The
726 connection between the syringe and the chip was realized by tygon tubing (Tygon S-54-HL,
727 inner diameter = 0.51 mm, outer diameter = 1.52 mm, VwR International GmbH, Germany) in
728 combination with blunt dispensing needles (General purpose tips, inner diameter = 0.41 mm,
729 outer diameter = 0.72 mm, Nordson EFD, USA). Medium flow was controlled by programmable
730 pressure regulators (LineUP FlowEZ, FLUIGENT, France), which generated flow by applying
731 pressure on 50-ml medium reservoirs (P-CAP series, FLUIGENT, France). Fresh and
732 conditioned TB medium were respectively filled in separate reservoirs, and each one was
733 pressurized by one module of the pressure regulator. After the cell inoculation both media were
734 connected to the inlets of the channel via tygon tubing and blunt dispensing needles. The
735 pressure at the inlet of the fresh TB medium was set to 200 mbar and remained constant
736 throughout the experiment. During the selection of the positions for imaging the pressure at
737 the inlet of the conditioned medium was set to 250 mbar, allowing the conditioned medium to
738 flow through the junction to the mother machine growth sites and thereby maintaining the
739 stationary state of the cells. At the beginning of imaging, the pressure at the inlet of the
740 conditioned medium was reduced to 150 mbar and programmed to increase back to 250 mbar
741 after 4 hours of on-chip cultivation, thereby activating a medium switch from fresh to
742 conditioned TB medium. Phase contrast and GFP fluorescence images were acquired with a
743 time interval of 10 min.

744

745 **Analysis of microfluidics data.** Cells were segmented from phase contrast images by
746 making use of a fully convolutional neural network based on the U-net architecture [2]. A set
747 of manually curated cell outlines was prepared for training (1105 outlines) and validation (346
748 outlines) of the network. The training set was augmented by scaling, rotation, flipping and
749 addition of white noise. A U-net of depth three, with 8, 16 and 32 filters along the contracting
750 path, was trained to predict cell interiors from phase contrast images. Phase contrast images
751 were normalized by subtracting the median and scaling to intensities expected between the
752 2^{nd} and 98^{th} percentiles. Cell interiors were defined from the curated outlines by filling each
753 outline and then subjecting it to two rounds of morphological erosion. The erosion step ensured
754 that neighbouring cells predicted by the network were well separated, such that distinct cell
755 instances could be clearly identified simply by thresholding the prediction and labelling

connected regions. After instance identification, two rounds of morphological dilation restored each mask to its original size. Finally, a smooth outline for each cell was obtained as a two-dimensional spline defined by equidistant knots placed on the mask edge.

To track cells between time points, we applied a length conservation strategy for the cells along each trench. At each time point, we ordered cell outlines by their depth in the trench, with deepest cells first. We then attempted to match, in order, a cell outline in time point *t* with one or more cell outlines in time point *t*+1, chosen such that the sum of their cell lengths would be conserved within some threshold tolerance. In the trivial case, the length of the first outline at time point *t* would match that of the first outline at time point *t*+1. In the event of cell division, the cell length at time point *t* would match the sum of the first two cell lengths at time point *t*+1. Since cells may grow in length between time points, we also initialised a growth rate parameter for each cell that biased the expected cell lengths for time point *t*+1 as a fold-increase in length. To enable adaptation to the true growth rate, the growth rate parameter was updated by a lagging average over 20 time points. To increase robustness to errors in segmentation, we additionally allowed state transitions from one to many and many to one, and built a proposal tree, which branched for all valid assignments lying within the length thresholds. We searched for the proposal with the lowest average fold-change in matched lengths, but limited branching by retaining only the 10 best proposals for subsequent nodes (cell outlines) in the tree. The length thresholds were deliberately set loosely such that the (sum of) cell length(s) at *t*+1 could decrease at most five-fold or increase at most two-fold relative to the (sum of) cell length(s) at *t*. This increased the number of valid proposals, but was important in cases where the growth rate estimate was poor. For transitions where one cell outline split into more than two, or transitions where multiple outlines merged into one cell, a new label was generated for the corresponding cells at *t*+1. We made one exception to this labelling strategy to account for occasional ambiguity in segmentation near division events, where a cell segmented as two sister cells could later be segmented as a single mother cell. Specifically, when two sister cells — i.e., cells that were previously involved in a division event — merged into one, the label was set back to that of the mother; at the next division event, the labels of the sister cells were also retained. Finally, note that any outlines below a minimum size threshold of 50 pixels were ignored. All errors in tracking were manually curated.

Cell length was estimated from cell regions as the ‘major axis length’ of the Matlab regionprops function — the major axis of the ellipse with same normalised second central moment as the region. Instantaneous growth rates were estimated from the derivative of a smoothing spline fitted to the logarithm of cell length over each cell division cycle. Knots for the spline were placed at intervals of at least 15 time points. Single-cell fluorescence traces were quantified from the median fluorescence within each outline. Background fluorescence varied as a function of time due to the accumulation of cells at some trench exits, so we corrected for

793 background fluorescence in each trench at each time point using the median value of all non-
794 cell pixels. Fluorescence traces were characterised along branching lineages and were
795 smoothed with a Savitzky-Golay filter of order 3 and window length 21. The derivative of the
796 filter was used to obtain the maximum rate of fluorescence increase. In cases where multiple
797 descendants shared a common peak event before branching, we counted that event only once.
798

799 **References**

800 1. Qin D, Xia Y, Whitesides GM. Soft lithography for micro- and nanoscale patterning. Nat
801 Protoc. 2010;5(3):491-502. Epub 2010/03/06. doi: 10.1038/nprot.2009.234. PubMed PMID:
802 20203666.
803 2. Ronneberger O, Fischer P, Brox T. U-net: Convolutional networks for biomedical image
804 segmentation. arXiv. 2015;[1505.04597].
805